

Biological effects of shielding parameters across the Bragg curve of energetic charged particles

Larry H. Rohde and Honglu Wu

ABSTRACT—Space radiation is a complex mixture of charged particles of solar and galactic origin. Many of these high-energy charged particles can penetrate current spacecraft shielding and produce secondary particles, creating significant health hazards. Therefore, understanding the biological effects of these particles along the particle traversal is critical to optimizing new shielding designs. The goal of this project is to obtain a distribution of biological damage as a function of the penetration depth for exposure to energetic charged particles by assessing the induction of micronuclei, a well-established biomarker for radiation exposure associated with chromosomal deletions. We aim to study the “biological Bragg curve” for a relevant number of particle types of varying energies, thus covering a broad LET spectrum. The rapidity, efficiency, and positional-preservation capability of the micronuclei assay will allow the practical analysis for our projected sample size.

INTRODUCTION

Space radiation is undoubtedly a major health concern for astronauts during cosmic missions, and especially during long-term interplanetary flights. The environment in space is a complex mix of many different types of ionizing and non-ionizing radiation that can be resolved into three broad categories:^{1,2} trapped particle radiation, solar particle radiation, and galactic cosmic radiation (GCR). Approximately 87 percent of the particles in the GCR spectrum are protons, 12 percent are helium nuclei, and 1 percent are particles heavier than helium, often referred to as high-Z and high-energy (HZE) particles. The heaviest biologically important of these HZE particles is iron because of its relatively large contribution to radiation dose and high LET.^{1,2} Understanding the extent and pattern of DNA damage induced by such particles in human cells is of primary importance for determining the associated biological risks and ensuring successful space exploration.³

Currently, the only major protection from space radiation available to astronauts is the shielding material of the space vehicle. Effective shielding of personnel and equipment from HZE particles (especially in the GCR spectrum) is a difficult task. Thin shielding has been shown to reduce dose equivalent as compared to no shielding. Unfortunately, shielding effectiveness drops as shielding thickness increases.⁴ This decrease in shielding effectiveness is due to the production of secondary particles (including neutrons) in the shielding material by primary GCR particles. In addition, unlike low-LET gamma or X-rays, the presence of shielding does not always reduce the radiation risks for energetic charged particle exposure. Heavy charged particles passing through shielding material will result in an energy loss of the particles as a function of their residual range, with the peak energy loss occurring as particles reach the end of their range,⁵ at which point the highest dose is deliv-

ered⁶ in the traversed material. This fragmentation modifies the quality of the incident beam and results in a Bragg curve distribution consisting of a mixed radiation field including primary particles and secondary fragments. Biophysical models are commonly used for evaluating the effectiveness of shielding in reducing biological damage and consequently designing spacecraft shielding.⁷⁻¹⁰ However, it is increasingly acknowledged that biological measurements¹¹ are urgently needed to validate the predictions resulting from these computer codes.

To date, studies involving the effects of shielding on radiation-induced biological outcomes have been few and far between. The U.S. National Academy of Sciences has determined that research on shielding composition and thickness using biological measurements should be a high priority for optimizing space radiation protection during deep space missions.¹² Some experiments aimed at studying the influence of shielding on biological effectiveness of high-energy iron (Fe) ions have been reported.^{13,14} However, little is known about the response using other biological end-points, and more important, the response occurring in the Bragg peak region of high LET radiation has been largely unclear. This may largely be due to a lack of suitable experimental designs that would allow the study of such phenomena with sufficient feasibility. Ground-based studies to investigate such matters would require a Bragg curve exposure of a continuous layer of biological sample within the radiation field and furthermore would necessitate the analysis of a biological end-point directly in real-time across this distribution without compromising positional status of the cells.

We thus proposed to design just such an experimental scheme, which would allow us to study the biological effects occurring across a Bragg curve distribution with a suitable biological end-point that would facilitate real-time analysis with sufficient resolution. The formation micronuclei is our

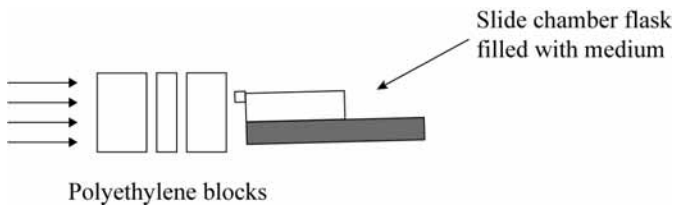


Figure 1. Schematic representation of the irradiation setup to achieve a Bragg curve distribution

biomarker of choice and is one of the most commonly used methods for measuring radiation-induced DNA damages.¹⁵⁻¹⁸

METHODOLOGY

Cell culture and irradiation. Immortalized human fibroblast cells (AG1522) cells were cultured in α -MEM media supplemented with 10 percent fetal bovine serum in a humidified incubator with 5 percent CO₂ at 37°C. Exponentially growing cells in chamber slides were covered with media and exposed to 138 MeV protons at a 0.5 or 2 Gy entrance dose, using the accelerator at Loma Linda University Medical School, Loma Linda, California. Polyethylene blocks of varying thicknesses were placed in front of the biological samples. The chamber slide was oriented such that the beam was almost parallel to the mono layer of the cells, as shown in Figure 1. After irradiation, excess media were removed and cells were incubated in fresh media containing cytochalasin-B for 48 hours. Slides were then washed with PBS and fixed with methanol/acetic acid (3:1).

Micronuclei and apoptosis assay. Slides were stained with 4-foot, 6-diamidino-2-phenylindole (DAPI) for analysis of MN using fluorescence microscopy by scanning in 1 mm increments across the length of slide to obtain data across the Bragg curve. About 1,000 cells were scored from each data point in a strip 1 mm wide across the distribution to generate data across the Bragg curve (depth-dose distribution curve). Multiple data points were generated within each slide, spanning a 5 cm area. MNs were identified only in bi-nucleated cells following the standard criteria.¹⁹ The total numbers of mono- and bi-nucleated cells were also counted, and the ratio of mono- to bi-nucleated cells was presented as an indicator of cell cycle progression, as previously reported.²⁰

RESULTS

The physical Bragg curve of 138 MeV protons was measured with polyethylene blocks and is shown in Figure 2. The residual range of the particles is about 13.5 cm in water. The dose remained constant in the entrance region and rose sharply as the particles approached the Bragg peak. Beyond the Bragg peak, the dose decreased sharply, as expected, from medium-energy protons. The chamber slides occupied the region of 9-17 cm from the beam entrance and covered the location of the Bragg peak (Figure 2). The MN frequency and the ratio of mono- to bi-nucleated cells are plotted against Bragg curve location for both entrance doses. Both the ratio of mono- to bi-nucleated cells and the MN frequency increased sharply at the Bragg peak, which resembled closely the physical Bragg curve distribution for both entrances doses.

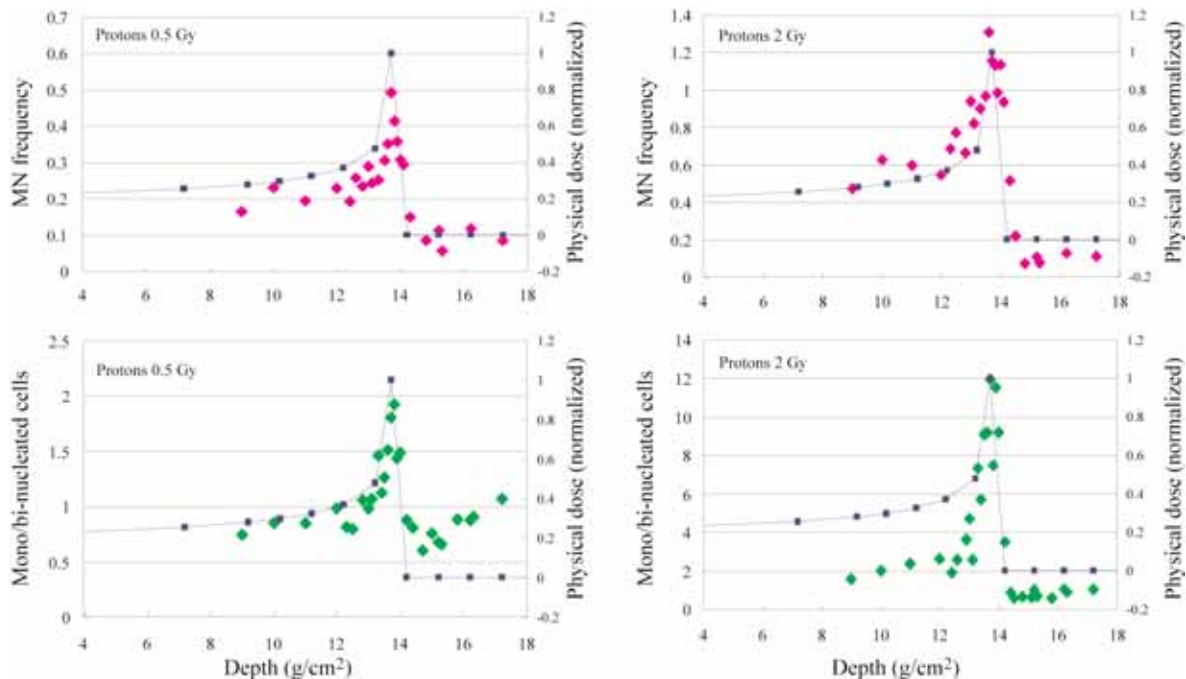


Figure 2. Yield of micronuclei, ratio of mono- to bi-nucleated cells and measured physical dose across the Bragg curve distribution for 138 MeV/nucleon protons. The entrance dose was 0.5 Gy and 2 Gy, and depth was converted to g/cm².

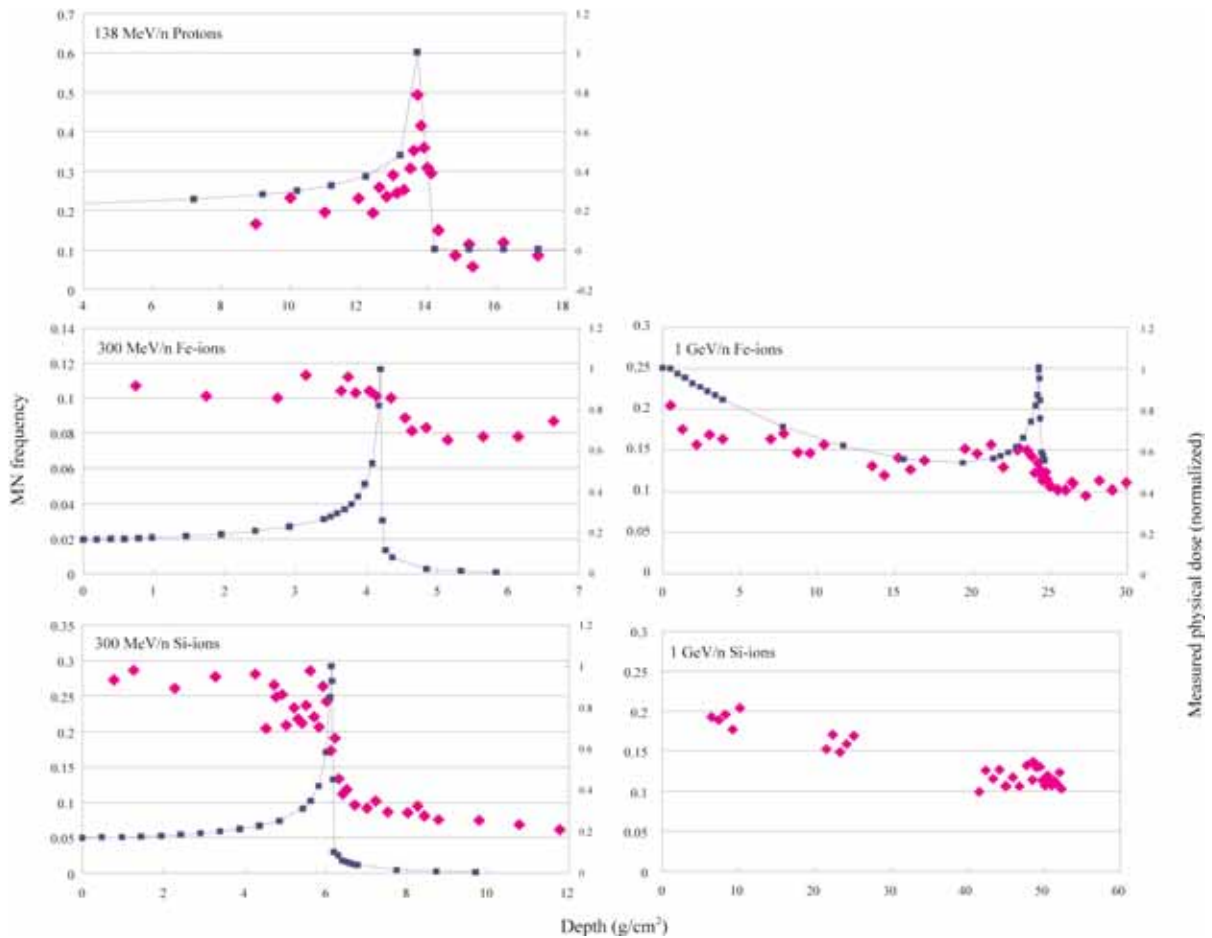


Figure 3. Micronuclei frequency and measured physical dose across the Bragg curve distribution for 138 MeV/nucleon protons, 300 MeV/nucleon Fe-ions, 1 GeV/nucleon Fe-ion, 300 MeV/nucleon Si-ions and 1 GeV/nucleon Si-ion. The entrance dose was 0.5 Gy, and depth was converted to g/cm². Only incident protons, and not Si and Fe ions, induced a peak of MN at the Bragg peak position.

DISCUSSION

Understanding of “biological Bragg curves” for the biological endpoints of interest is essential in designing effective shielding strategies for space radiation protection and in planning charged particle radiotherapy. Recently, we have performed a series of experiments to study H2AX phosphorylation and MN induction around the Bragg peak region.^{20,21} In a previous study with entrance Si and Fe ions of the same entrance doses as in the present study,²⁰ we did not observe an increase in the MN yield around the Bragg peak (Figure 3). However, the ratio of mono- to bi-nucleated cells resembled the physical Bragg curve closely for the two heavy ion types (Figure 3). These results with Si and Fe ions confirmed the hypothesis that “overkill” at the Bragg peak will affect the outcome of other biological endpoints that require cell cycle progression. Our present study with protons demonstrated clearly that the degree of resemblance of physical and biological Bragg curves, particularly in the Bragg peak region, depends highly upon the particle types (Figure 3). While the ratio of mono- to bi-nucleated cells, which is relevant to cell cycle progression and cell death, increased at the location of the Bragg peak for both light and heavy ions, only protons, and possible

other light ions, showed a “biological Bragg peak” for MN induction. We plan to carry out similar studies with helium and carbon ions that fill the gap between protons and the heavy ions.

REFERENCES

1. Guidance on Radiation Received in Space Activities. Report 98. Bethesda, MD: National Council on Radiation Protection and Measurements (1989).
2. Radiation Protection Guidance for Activities in Low Earth Orbit. Report 132. Bethesda, MD: National Council on Radiation Protection and Measurements (2000).
3. Goodhead, D.T. The initial physical damage produced by ionizing radiations. *Int. J. Radiat. Biol.* **56**, 623-634 (1989).
4. Badhwar G.D. and Cucinotta F.A. A comparison of depth dependence of dose and linear energy transfer spectra in aluminum and polyethylene. *Radiat Res.* **153**, 1-8 (2000).
5. International Commission on Radiation Units and Measurements, ICRU Report 16, Linear Energy Transfer, International Commission on Radiation Units and Measurements, Washington, June 15 (1970).
6. Turner, J.E. *Atoms, Radiation, and Radiation Protection*.



Photo courtesy of Larry Rohde

MICROSCOPY—Ye Zhang, ISSO post-doctoral aerospace fellow, uses fluorescence microscopy to study micronuclei and apoptosis in experimental samples.

(McGraw-Hill, Inc., New York, 1992).

7. Wilson, J.W., Thibeault, S.A., Cucinotta, F.A., Shinn, J.L., Kim, M., Kiefer, R., and Badavi, F.F. Issues in protection from galactic cosmic rays. *Radiat. Environ. Biophys.* **34**, 217-222 (1995).
8. Wilson, J.W., Miller, J., Konradi, A., and Cucinotta, F.A. (Eds.) *Proceedings, Shielding Strategies for Human Space Exploration*. NASA-Johnson Space Center, Houston, TX, NASA CP-3360 (Dec. 6–8, 1995). (NASA-Langley Research Center, Hampton, VA, 1997).
9. Wilson, J.W., Cucinotta, F.A., Kim, M.H., and Schimmerling, W. Optimized shielding for space radiation protection. *Phys Med.* **17**, S67-S71 (2001).
10. Wilson, J.W., Tripathi, R.K., Qualls, G.D., Cucinotta, F.A., Prael, R.E., Norbury, J.W., Heinbockel, J.H., Tweed, J., and De Angelis, G. Advances in space radiation shielding codes. *J. Radiat. Res.* **43**, S87-S91 (2002).
11. George, K., Willingham, V., Wu, H., Gridley, D., Nelson, G., Cucinotta, F.A. Chromosome aberrations in human lymphocytes induced by 250 MeV protons: Effects of dose, dose rate and shielding. *Adv. Space Res.* **30**, 891-899 (2002).
12. National Academy of Sciences, Radiation Hazards to Crews on Interplanetary Missions. Report of the Task Group on the Biological Effects of Space Radiation. (National Academy Press, Washington DC, 1997).

13. Durante, M., Gialanella, G., Grossi, G., Pugliese, M., Scampoli, P., Kawata, T., Yasuda, N., and Furusawa, Y. Influence of the shielding on the induction of chromosomal aberrations in human lymphocytes exposed to high-energy iron ions. *J. Radiat. Res.* **43** Suppl, S107-11 (2002).
14. Grossi, G., Durante, M., Gialanella, G., Pugliese, M., Scampoli, P., Kawata, T., Yasuda, N., and Furusawa, Y. Chromosomal aberrations induced by high-energy iron ions with shielding. *Adv. Space Res.* **33**, 2004.
15. Hall, E.J and Hei, T.K. Genomic instability and bystander effects induced by high-LET radiation. *Oncogene* **13**, 7034-42 (2003).
16. Shao, C., Furusawa, Y., Kobayashi, Y., Funayama, T., and Wada, S. Bystander effect induced by counted high-LET particles in confluent human fibroblasts: A mechanistic study. *FASEB J.* **17**, 1422-7 (2003).
17. Akudugu, J.M., Slabbert, J.P., Roos W.P., and Bohm, L. Micronucleus response of human glioblastoma and neuroblastoma cells toward low-LET photon and high-LET p(66)/Be neutron irradiation. *Am J Clin Oncol.* **26**, 1-6 (2003).
18. Oliveira, N.G., Castro, M., Rodrigues, A.S., Concalves, I.C., Gil, O.M., Fernandes, A.P., Toscano-Rico, J.M., and Rueff, J. Wortmannin enhances the induction of micronuclei by low and high LET radiation. *Mutagenesis* **18**, 217 (2003).
19. Fenech, M. and Morley, A.A. Cytokinesis-block micronucleus method in human lymphocytes: Effect of *in vivo* ageing and low dose x-irradiation. *Mutat Res.* **161**, 193-8 (1986).
20. Wu, H., Hada, M., Meador, J., Hu, X., Rusek, A., and Cucinotta, F.A. Induction of micronuclei in human fibroblasts across the Bragg curve of energetic heavy ions. *Radiat Res.* **166.4**, 583-589 (2006).
21. Desai, N., Durante, M., Lin, Z.W., Cucinotta, F.A., and Wu, H. High LET—induced H2AX phosphorylation around the Bragg curve. *Adv. Space Res.* **35**, 236 (2005).

FUNDING AND PROPOSALS

Validation of a terrorist attack radiation biodosimeter: Practical application of an optimized gamma-H2AX assay, National Institutes of Health, \$1,174,232 (Sept. 2008–Sept. 2012).

Treatment of radiation burns by transient siRNA knock-down of genes induced by ionizing radiation, National Institutes of Health, \$971,052 (Sept. 2008–Sept. 2012).